Journal of
Materials Sciences and Applications

Research Article Open Access

Thermolysis Products of Double Complex Compounds as Precursors of Metal--Carbon Composites

Denis P. Domonov* and Sofia I. Pechenyuk

I.V. Tananaev Institute of Chemistry and Technology of Rare Elements and Mineral Raw Materials of RAS KSC (ICTREMR), Akademgorodok, 26a, Apatity, Murmansk region 184209, Russia

***Corresponding Author:** Denis P. Domonov, I.V. Tananaev Institute of Chemistry and Technology of Rare Elements and Mineral Raw Materials of RAS KSC (ICTREMR), Akademgorodok, 26a, Apatity, Murmansk region 184209, Russia, E-mail: d.domonov@ksc.ru

Received Date: September 23, 2024 **Accepted Date:** October 23, 2024 **Published Date:** October 26, 2024

Citation: Denis P. Domonov, Sofia I. Pechenyuk (2024) Thermolysis Products of Double Complex Compounds as Precursors of Metal-Carbon Composites. J Mater sci Appl 8: 1-10

Abstract

Thermal decomposition of double complex compounds of 3d metals in argon atmosphere in the temperature region 200-900°C has been studied. It was found that at temperatures >600°C metal-carbon composites are formed. Their composition, thermal stability, specific surface area and crystalline modification were investigated. Treatment of the composites with acids allows to obtain products with a developed surface and increased content of carbon, which is largely graphitised. The obtained composites are stable when heated in air up to 450-500°C and completely burn up to 700°C.

Keywords: Complex Compounds; Thermolysis; Argon; Metal-Carbon Composites

Introduction

Currently, a large number of works of modern research are devoted to the creation of nanocomposite structures, which are formed by mixing one or more heterogeneous materials at the nanoscale, which allows obtaining objects with improved properties. Nanocomposites demonstrate superhydrophobicity, superhydrophilicity, thermal energy transfer, electronic and ionic transport, resistance to abrasion and contamination, which makes them attractive for obtaining electrochemical capacitors [1-3], catalysts [4-6], sensors [7-9], adsorbents [10-13], etc.

Nanocomposites are interesting from the point of view of protecting human health and the normal functioning of electronic devices due to the increasing electromagnetic pollution of the environment [14,15]. We need materials, on the one hand, capable of converting electromagnetic energy into thermal energy, and on the other hand, absorbing microwave radiation and able to solve the problem of electromagnetic interference. The composite should consist of magnetic and dielectric components, since dielectric permittivity and magnetic permeability are complementary; have lightweight and strong absorption in a wide frequency band. Fe, Co and Ni combined with carbon have such properties.

The task of the process of obtaining such materials is to introduce metals into dispersed carbon, so that they would be uniformly distributed throughout the volume of carbon and in their dispersion would be close to it. For example, a method for the preparation of Co-Fe-C composites using an alginate fiber substrate was described, where sodium alginate and cobalt and iron chlorides were the starting products [16], impregnation of the fiber with cobalt and iron in a water-ethanol solution under the action of ultrasound, washing, drying and carbonization of the sample in an argon atmosphere. In [17], electrodeposition method was used to obtain a similar Co-Fe-C composite. The authors [18] prepared FeCo-C nanofilaments by electrospinning from solutions of iron and cobalt acetylacetonates in dimethylformamide. In [19,20], metal nanoparticles embedded in porous carbon composites were synthesized by calcination of a mixture of organic carbon and metal nitrates. They were uniformly dispersed in the porous carbon matrix. The complex dielectric constant of Cu/C nanocomposites can be tuned by varying the Cu:C ratio. Obtaining composites with foam structure is a separate direction in the development of metal-carbon materials and has been widely investigated [21,22].

The analysis of literature data shows that obtaining bimetallic composites is associated with a number of sequential operations aimed at bringing metal ions into contact with the organic framework, which must then be converted into carbon with simultaneous reduction of metal ions. If carbides are introduced into the organic phase, the synthesis of these carbides themselves is a complex challenge in its own right.

Previously we investigated the thermal decomposition of double complex compounds (DCCs). It was necessary to take into account the influence of the external gas atmosphere on the thermolysis process, so part of the work was the study of thermolysis in an inert atmosphere. It was found that some amount of carbon always remains in the solid residue from the calcination of most of the DCCs [23,24]. Consequently, such compounds can be used as precursors of metal-carbon compositions, which have not been previously considered in the literature. The method is characterized by simplicity, since it consists of two steps: synthesis of DCCs and thermolysis in an inert atmosphere. Ultimately, this leads to the formation of high-mogeneous materials and a decrease in the calcination temperature, i.e., a reduction in energy consumption compared to traditional methods of production. This paper describes the conditions of production and properties of new metal-carbon materials.

Experimental Section

The first step is the synthesis of DCS [24]. Then, guided by TG and DTG curves obtained in argon atmosphere, we selected the required temperatures for thermolysis.

A sample of DCC was placed in a tubular quartz reactor inserted into a NaberthermRT 50-250/11 tube furnace (Nabertherm GmbH, Lilienthal, Germany), heated in an argon current at a rate of 10/min and kept at the desired temperature for one hour, after which it was cooled in an argon

atmosphere to room temperature. In order to study the mechanism of thermolysis, the gaseous products of thermolysis were captured and tried to identify, and the solid products were subjected to physical and chemical investigation: elemental analysis, IR spectrometry, X-ray diffraction analysis, specific surface area measurement.

Elemental analysis, X-ray diffraction (XRD), IR spectroscopy and electron microscopy were used to study the DCC and the products of their thermolysis. Analysis for carbon content was performed on an ELTRA CS-2000 automatic analyzer (Alpha Resources, LLC, and Stevensville, MI, USA). To determine the metal content, weighed portions of the complex or the products of its thermolysis were dissolved in a mixture of concentrated acids HNO_3 and HCl. The resulting solutions were analyzed by the atomic absorption method on an Analyst 400 spectrometer (PerkinElmer, Inc. Waltham, MA, USA). Diffraction patterns were obtained on a Shimadzu XRD 6000 diffractometer (Shimadzu Corp., Columbia, MD, USA) (using CuKα radiation (graphite monochromator, λ = 1.54Å) and compared with the data of the JCPDS-ICDD 2002 database.

The specific surface areas of thermolysis products were measured using Tristar 3020 and FlowSorb2300 devices from Micromeritics (Micromeritics Instrument Corp. Norcross, GA, USA).

Thermal analysis of the initial DCC was carried out in an argon atmosphere on a NETZSCH STA 409 PC / PG device (NETZSCH-Geratebau ¨GmbH, Selb, Germany), sample weighed amount 7-10 mg, heating rate 10°/min, temperature range 20-1000°C.

Scanning electron microphotographs were obtained using a SEM Leo 420 instrument (LEO, Assing, Italy).

Results and Discussion

Thermal decomposition in argon was carried out for the following compounds: $[Co(NH_3)_6][Fe(C_2O_4)_3]\cdot 3H_2O$ $[Ni(NH_3)_6]_3[Fe(CN)_6]_2$, $[Co(en)_3][Fe(C_2O_4)_3]$, $[Co(NH_3)_6][Fe(CN)_6]$, $[Co(NH_3)_6]_4[Fe(CN)_6]_3\cdot 13H_2O$, $[Co(en)_3][Fe(CN)_6]$, $[Co(en)_3]_4[Fe(CN)_6]_3\cdot 15H_2O$, $[Co(NH_3)_6]Cl$ $[Cu(C_7H_4O_3)_2]\cdot 3H_2O$. Similar composites were also obtained from DCCs with aqua complexes in the cation: $[Cu_{aq}]_3[Fe(Co)(CN)_6]_2\cdot 15H_2O$ and $[Ni_{aq}]_3[Fe(Co)(CN)_6]_2\cdot 16H_2O$.

The composition of residues from calcination (primary composites), their specific surfaces, temperature of obtaining, and morphology of particles are given in Table 1, the corresponding data for secondary composites - in Table 2.

Table 1: Characteristics of primary composites

Initial complex	T, °C	CompositionMe/C	Ratio Me_1:Me_2:C	S_{sp}, m^2/g	Morphology
$[Co(en)_3][Fe(ox)_3]$	550	60,7/23,6	1:0,9:3,6	93	hollow prisms
	600	63,7/21,2	1:1:3	154	
	700	71,2/23	1:0,9:2,9	128	
$[Ni(NH_3)_6]_3[Fe(CN)_6]_2$	600	77/23	3:2:7,3	27,7	fine tangled filaments + spongy aggregates
	650	78/22	3:2:7	43,8	
	700	80/19	3:2:5,5	72,7	
	800	72,9/21,6	3:2:7	78,5	
$[Co(NH_3)_6][Fe(CN)_6]$	630	71/29	1:1:3,9	36,5	rod-like particles
	800	70,8/27,5	1:1:3,7	35,7	
$[Co(NH_3)_6]_4[Fe(CN)_6]_3$	675	75,3/22,1	4:3:9,7	48	spongy masses

	950	76/23	4:3:10,1	49,3	
$[Co(en)_3][Fe(CN)_6]$	450	39/30	1:1:7,4	22	elongated nodules
	700	60/40	1:1:6,5	–	
$[Co(en)_3]_4[Fe(CN)_6]_3$	560	55/30	4:3:18,4	33	irregularly shaped debris
	650	64,5/35	4:3:17,9	102	
$[Co(NH_3)_6]Cl[Cu\ (C_7H_4O_3)_2]$	650	57,6/29	1:1:5,2	38.6	porous cellular formations
	900	67,7/33	1:1:5	186	

Table 2: Characteristics of secondary metal-carbon composites

Initialcomplex	T, C	Yield, g C/g complex	ContentMe_1+Me_2, %	S_{sp}, m^2/g	d (S_{sp}), nm	d (Scherrer formula), nm	Morphology
$[Co(en)_3][Fe(ox)_3]$	550	0,37		255	15		Hollow prisms
	600	0,36		263	15		
	700	0,45		328	12		
$[Ni(NH_3)_6]_3[Fe(CN)_6]_2$	600	0,30		224	14		Filamentous crystals
	650	0,24	4,2 + 3,4	226	17	36	
	700	0,28	8,0 + 6,8	276	14	14	
	800	0,33	8,4 + 6,1	230	17	40	
$[Co(NH_3)_6][Fe(CN)_6]$	630	0,32	3,8 + 4,8	109	29	31	Tubular particles
	800	0,31	2,3 + 3,0	109	31	31	
$[Co(NH_3)_6]_4[Fe(CN)_6]_3$	675	0,31	13,0 + 11,0	176	22	22	Fine filament conglomerate
	950	0,31	11,6 + 9,4	150	26	26	
$[Co(en)_3][Fe(CN)_6]$	450	0,31	13,3 +14,6	380	–	–	Sponge plates
	700	0,61	13,0 +10,4	230	11	9	
$[Co(en)_3]_4[Fe(CN)_6]_3$	560	0,46	25,4 +9,5	40	–	–	Irregularly shaped debris
	650	0,52	16,4 +10,7	206	11	13	
$[Co(NH_3)_6]Cl[Cu(C_7H_4O_3)_2]$	650	0,46	17	48	53	–	Large porous particles
	900	0,33	undetected	466	8	–	

[1]In Table 1 and 2 crystallization water is not specified

In the course of studies, we found that $[Co(NH_3)_6][Fe(C_2O_4)3]\cdot 3H_2O$ does not form a composition with carbon during thermolysis in argon, that is, the oxalate complex completely decomposes with the release of carbon oxides. It seems that in the case of $[Co(en)_3][Fe(C_2O_4)_3]$ the residual carbon arises at the expense of the cation. However, we further see a number of hexacyanoferrate and hexacyano-cobaltate DCCs whose cations do not contain carbon and which, however, form carbon-rich compositions. Consequently, the carbon source here is anions, more precisely, cyanogroup ligands or salicylate.

It is well seen (Table 1) that the main component of the primary composites are metal-complexing agents, the content of which can reach 80 wt%. The content of carbon is usually in the range of 20-30 wt. %, in some cases it reaches 35-40 wt. %. The ratio of elements indicates that the carbon content usually decreases gradually with increasing thermolysis temperature. The specific surface area of the primary composites increases with increasing temperature, sometimes having a maximum, as for example in the case of $[Co(en)_3][Fe(ox)_3]$. If the initial DCS consists of relatively small ligands (NH_3, CN-groups), the specific surface of thermolysis products does not exceed 80 m^2/g. In the case of compounds with large ligands (ethylenediamine, oxalate, salicylate), the specific surface area can reach 186 m^2/g. This is also reflected in the morphology. Thermolysis of the most "compact" complexes $[Co(NH_3)_6][Fe(CN)_6]$ and $[Co(en)_3][Fe(CN)_6]$ leads to the formation of rod-shaped oblong particles repeating the shape of the original crystals, which have the smallest surface area and probably the highest density among the studied composites. If the ratio of metals in the cation and anion is 4:3, we are initially dealing with less dense structures that are penetrated by channels with a large amount of crystallization water. This leads to the appearance of irregularly shaped spongy particles during thermolysis. Complex organic ligands, such as salicylate, produce a developed surface in the form of highly porous particles upon thermolysis in argon. This can be useful in those practical applications where specific surface area plays an important role, such as in catalysis.

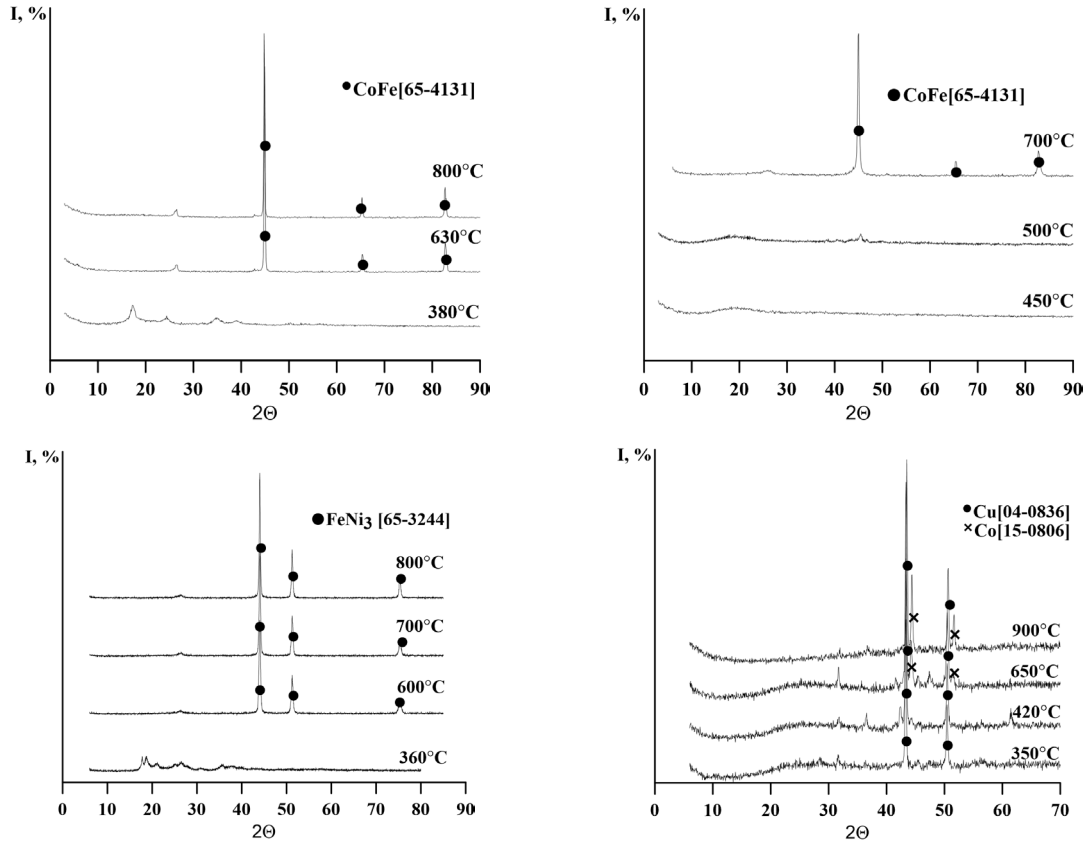

Figure 1: XRD patterns of thermolysis products in argon (primary composites): a) $[Co(NH_3)_6][Fe(CN)_6]$; b) $[Co(en)_3][Fe(CN)_6]\cdot 2H_2O$; c) $[Ni(NH_3)_6]_3[Fe(CN)_6]_2$, d) $Co(NH_3)_6]Cl[Cu(C_7H_4O_3)_2]\cdot 3H_2O$.

XRD patterns of metal-carbon primary composites obtained by thermolysis of DCCs in argon atmosphere are shown in Figure 1. For the products obtained at high temperatures we see characteristic peaks (2Θ = 43-45; 65; 83°) corresponding to CoFe alloy and a very weak peak (2Θ = 23-26°) corresponding to carbon (Figure 1a, b). A similar XRD patterns were observed in [16,17] for CoFe/C composites. In the case of CoCu compounds the carbon reflections are absent (Figure 1d).

The primary composites were treated with 6 M hydrochloric acid to remove metals from them. It is not always possible to do this at room temperature and in a single step. In addition, residues containing copper had to be additionally treated with nitric acid. Table 2 shows the characteristics of samples separated from primary composites by acid treatment - secondary composites.

It can be seen that the extracted products still contain a significant amount of metals. Equimolarity of metals is already broken here, the content of cobalt slightly exceeds the content of iron. The specific surface area value of the secondary composite is usually more than 2 times this value for the primary composite. It seems that the carbon envelops the metal particles and the acid treatment opens up these envelopes. The particle size was estimated using Scherrer's formula and S_{sp}.

When considering the morphology of carbon, it can be assumed that if carbon was absent in the cationic part of DCC, the secondary product is obtained as fibrous, and if present, it is in the form of shapeless particles. It is also seen that treatment of primary composites with acid allows to regulate the content of metals in them, as well as their specific surface area.

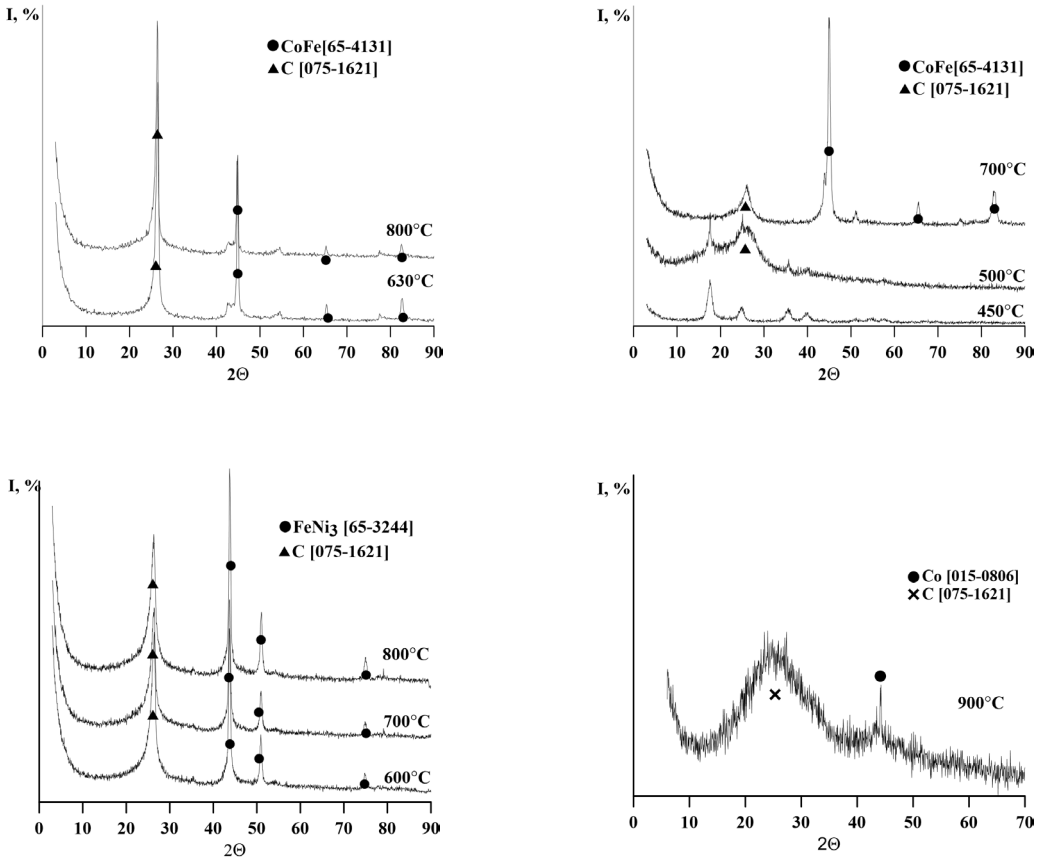

Figure 2: XRD patterns of secondary composites: a) $[Co(NH_3)_6][Fe(CN)_6]$; b) $[Co(en)_3][Fe(CN)_6]\cdot 2H_2O$; c) $[Ni(NH_3)_6]_3[Fe(CN)_6]_2$, d) $[Co(NH_3)_6]Cl[Cu(C_7H_4O_3)_2]\cdot 3H_2O$

Figure 3 shows the thermal analysis curves of the secondary NiFe/C composite and pure carbon, It can be seen how well the TG curves of both samples match. The properties of this composite are very similar to expanded graphite. It has a highly developed surface (276 m^2/g) and is

stable in air when heated up to 450°C.

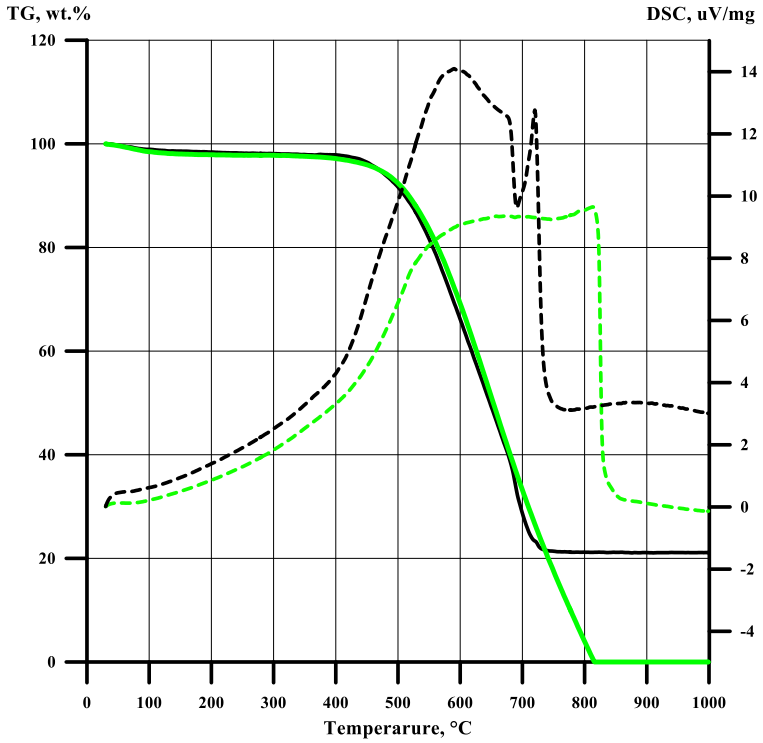

Figure 3: Thermal analysis curves in air atmosphere of the secondary composite of secondary composite $[Ni(NH_3)_6]_3[Fe(CN)_6]_2$_700C (▬) and carbon (▬).

Conclusion

Thermal decomposition of double complex compounds in argon leads to formation of products with carbon content up to 40 wt. % and specific surface from 20 to 190 m^2/g. Leaching with hydrochloric acid of a part of metals leads to a strong increase of specific surface up to 470 m2/g with residual content of the sum of metals 10-20%. XRD patterns of the primary composites show almost no carbon reflections in the region 2Θ = 20-30°, whereas the secondary composites show them perfectly. Thermolysis of double complex compounds allows to obtain metal-carbon composites at temperatures 600-900°C, while alternative methods of obtaining products with similar properties require synthesis conditions at 1500-2000°C. Further studies are planned to expand the set of DCCs precursors, conductivity measurements of composites at different emission frequencies and optimize the conditions for obtaining the most promising samples.

References

1. NPD Ngidi, AF Koekemoer, SS Ndlela (2024) Application of metal oxide/porous carbon nanocomposites in electrochemical capacitors: A review, Physics and Chem. of the Earth, Parts A/B/C, 135: 103698.

2. ER Ezeigwe, PS Khiew, CW Siong, MTT Tan (2020) Mesoporous Zinc–Nickel–Cobalt nanocomposites anchored on graphene as electrodes for electrochemical capacitorshttps, J. of Alloys and Compounds, 816: 152646.

3. GK Maron, JH Alano, BS Noremberg, LS Rodrigues, V Stolojan, SRP Silva, NLV Carreño (2020) Electrochemical supercapacitors based on 3D nanocomposites of reduced graphene oxide/carbon nanotube and ZnS, J. of Alloys and Compounds, 836: 155408.

4. ME Khan (2021) State-of-the-art developments in carbon-based metal nanocomposites as a catalyst: photocatalysis, Nanoscale Adv. 3: 1887-900.

5. TY Su, GP Lu, KK Sun, M Zhang, C Cai (2022) ZIF-derived metal/N-doped porous carbon nanocomposites: efficient catalysts for organic transformations, Catal. Sci. Technol. 12: 2106-21.

6. GW Woyessa, JB Cruz, M Rameez, CH Hung (2021) Nanocomposite catalyst of graphitic carbon nitride and Cu/Fe mixed metal oxide for electrochemical CO2 reduction to CO, App. Catalysis B: Environmental, 291: 120052.

7. C Zhang, L Li (2024) Study on electrochemical sensor for sunitinib cancer medicine based on metal-organic frameworks and carbon nanotubes nanocomposite, Alexandria Engineering J. 97: 8-13.

8. A Yadav, A Kumar, N Verma (2021) Microchannel–engraved and Cu–dispersed carbon nanocomposite film as a chemiresistive sensor for aqueous metal ions, Chemical Engineering Science, 231: 116282.

9. AI Ayesh, Z Karam, F Awwad, MA Meetani (2015) Conductometric graphene sensors decorated with nanoclusters for selective detection of Hg2+ traces in water, Sensors and Actuators B: Chemical, 221: 201-6.

10. J Nyirenda, G Kalaba, O Munyati (2022) Synthesis and characterization of an activated carbon-supported silver-silica nanocomposite for adsorption of heavy metal ions from water, Results in Engineering, 15: 100553.

11. T Hridya, V Emily, PS Harikumar (2021) Removal of heavy metals from aqueous solution using porous (Styrene-divinylbenzene)/CuNi bimetallic nanocomposite microspheres, Environmental Nanotechnology, Monitoring & Management, 16: 100606.

12. X. Zhang, W. Li, X. Wang, M. Su, Q. Lin, A novel 3D hierarchical NiFe-LDH/graphitic porous carbon composite as multifunctional adsorbent for efficient removal of cationic/anionic dyes and heavy metal ions, J. Molecular Liquids, 411: 125753.

13. Wk Li, Hx Zhang, Yp Shi (2017) Selective adsorption of aromatic acids by a nanocomposite based on magnetic carboxylic multi-walled carbon nanotubes and novel metal-organic frameworks, Applied Surface Science, 416: 672-80.

14. F Shahzad, M Alhabeb, CB Hatter, B Anasori, S Man Hong, CM Koo, Y Gogotsi (2016) Electromagnetic interference shielding with 2D transition metal carbides (MXenes), Science, 353: 1137-40.

15. H Lv, Z Yang, PL Wang, G Ji, J Song, H Zeng, ZJ Xu (2018) A voltage boosting strategy enabling a low-frequency, flexible electromagnetic wave absorption device, Adv. Mater. 30: 1706343.

16. Z Song, X Liu, X Sun, Y Li, X Nie, W Tang, R Yu, J Shui (2019) Alginate-templated synthesis of CoFe/carbon fiber composite and the effect of hierarchically porous structure on electromagnetic wave absorption performance, Carbon, 151: 36-45.

17. Y Wan, J Xiao, C Li, G Xiong, R Guo, L Li, M Han, H Luo (2016) Microwave absorption properties of FeCo-coated carbon fibers with varying morphologies, J. Magnetism and Magnetic Materials, 399: 252-9.

18. J Xiang, X Zhang, Q Ye, J Li, X Shen (2014) Synthesis and characterization of FeCo/C hybrid nanofibers with high performance of microwave absorption, Materials Research Bulletin, 60: 589-95.

19. X Du, B Wang, C Mu, F Wen, J Xiang, A Nie, Z Liu (2018) Facile Synthesis of Carbon-Encapsulated Ni Nanoparticles Embedded into Porous Graphite Sheets as High-Performance Microwave Absorber, ACS Sustain. Chem. Eng. 6: 16179-85.

20. Liu Sh, Du Xia, Xu J, Guo S (2020) Metal Copper nanoparticles embedded in porous carbon as high reflection loss absorbers of high frequency electromagnetic wave. // Solid State Communications, 312: 113876.

21. L Lyu, F Wang, X Zhang, J Qiao, C Liu, J Liu (2021) CuNi alloy/ carbon foam nanohybrids as high-performance electromagnetic wave absorbers, Carbon, 172: 488-96.

22. H Yang, B Wen, L Wang (2020) Carbon nanotubes modified CoZn/C composites with rambutan-like applied to electromagnetic wave absorption, Applied Surface Science, 509: 145-336,

23. SI Pechenyuk, DP Domonov, AA Shimkin, YuP Semushina, YuV Ivanov (2017) Thermal behavior of binary complex compounds containing the hexacyanoferrate anion, Rus. J. Gen. Chem. 87: 2212-23.

24. SI Pechenyuk, DP Domonov, AN Gosteva (2021) Thermal Decomposition of Cationic, Anionic, and Double Complex Compounds of 3d-Metals, Rus. J. Gen. Chem. 91: 1834-61.

25. MB Vazquez-Santos, E Geissler; K Laszlo, JN Rouzaud, A Martinez-Alonso, JMD Tascon (2012) Comparative XRD, Raman and TEM Study on graphition of PBO-derived Carbon Fibers, J. Phys. Chem. 116: 257-68.